ChemComm

Skeletal rearrangement of a boron-containing annulenic molecule into a macrocycle bridged by an electronically stabilized boron cation

Journal:	*ChemComm*
Manuscript ID	CC-COM-09-2023-004830.R1
Article Type:	Communication

ChemComm

COMMUNICATION

Skeletal rearrangement of a boron-containing annulenic molecule into a macrocycle bridged by an electronically stabilized boron cation†

Received 00th January 20xx,
Accepted 00th January 20xx

DOI: 10.1039/x0xx00000x

Yukihiro Murata,[a,b] Cihan Özen,[c,d] Satoshi Maeda,*[c,d] Takanori Fukushima[a,b,e] and Yoshiaki Shoji*[a,b]

An annulenic molecule containing a three-coordinate chloroborane moiety, which exhibits a borane-olefin proximity effect, undergoes a skeletal rearrangement upon chloride abstraction, to generate a three-dimensional macrocyclic molecule featuring a borocenium (η^5-cyclopentadienyl–B$^+$–R) structure.

Electron-deficient organoboron compounds when interacting with unsaturated C–C bonds can cause a variety of organic transformations. For example, the interaction between boranes and olefins results in uncatalyzed hydroboration.[1] Olefin activation by frustrated Lewis pairs (FLPs) is also categorized into this type of reaction.[2] Although borane-olefin complexes had been considered as weakly interacting van der Waals complexes,[3,4] it has recently been shown that they can affect the structure and reactivity of molecular systems having borane and olefinic moieties in close proximity.[5–8] Yamaguchi and coworkers reported a reversible FLP-type addition reaction of Lewis bases to an olefin-containing triarylborane derivative with a structure where borane and olefin moieties are close to each other.[6] Braunschweig and coworkers revealed that the boron-bridged boranorbornadiene derivatives formed in the reaction between a borole and an alkyne derivative are in equilibrium with borepins and boranorcaradienes in solution, due to intramolecular complexation between the borane moieties and the π-system.[7] There is growing understanding of interactions between borane and unsaturated C–C bonds in terms of their chemical reactivities. However, for cationic boron species having enhanced Lewis acidity, knowledge of their interactions with unsaturated C–C bonds, particularly, in relation to chemical reactivity still remains limited.[9–11] Here we show a unique skeletal rearrangement of an annulene-type molecule (Fig. 1, **3**$_{Cl}$), upon generating a cationic boron moiety by chloride (Cl^-) abstraction, where multiple C–C and C–B bonds cleavage and formation occur to give rise to a three-dimensional (3D) macrocycle featuring a borocenium (η^5-cyclopentadienyl–B$^+$–R) structure.

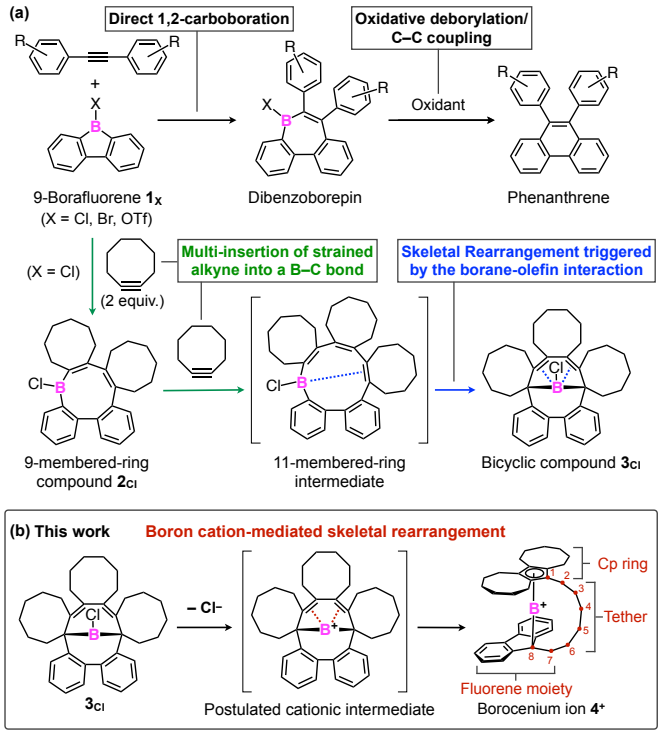

Fig. 1. (a) 1,2-Carboboration of alkynes with borafluorene **1**$_X$ to afford dibenzoborepin derivatives, and subsequent oxidative deborylation/C–C coupling that affords phenanthrene derivatives (top). Multi-insertion of cyclooctyne into the B–C bond of 9-borafluorene (X = Cl) to form boron-containing 9-membered-ring compound **2**$_{Cl}$ and bicyclic compound **3**$_{Cl}$ (bottom). (b) Boron cation-mediated skeletal rearrangement of a boron-containing annulenic molecule.

[a] *Laboratory for Chemistry and Life Science, Institute of Innovative Research, Tokyo Institute of Technology, 4259 Nagatsuta, Midori-ku, Yokohama 226-8503, Japan* E-mail: yshoji@res.titech.ac.jp (Y.S.)
[b] *Department of Chemical Science and Engineering, School of Materials and Chemical Technology, Tokyo Institute of Technology, 4259 Nagatsuta, Midori-ku, Yokohama 226-8503, Japan*
[c] *Institute for Chemical Reaction Design and Discovery (WPI-ICReDD), Hokkaido University, Sapporo 060-8510, Japan,* Email: smaeda@eis.hokudai.ac.jp (S.M.)
[d] *Department of Chemistry, Hokkaido University, Sapporo 060-8510, Japan*
[e] *Living Systems Materialogy (LiSM) Research Group, International Research Frontiers Initiative (IRFI), Tokyo Institute of Technology, 4259 Nagatsuta, Midori-ku, Yokohama 226-8503, Japan*

†Electronic Supplementary Information (ESI) available: Experimental and crystallographic details and analytical data. CCDC-2297987 (**4**$^+$[$(C_6F_5)B]^-$), CCDC-2297988 (**5**) and CCDC-2297989 (**6**). For ESI and crystallographic data in CIF or other electronic format, see DOI: 10.1039/x0xx00000x

Figure 1 shows the overall picture of the reactions reported herein. The boron-containing macrocycle ($\mathbf{3}_{Cl}$) was obtained in the course of our previous study on alkyne activation reactions with cyclic boranes.[8,12] We have reported direct 1,2-carboboration reactions between 9-borafluorene $\mathbf{1}_{X}$ ($\mathbf{1}_{Cl}$: X =Cl, $\mathbf{1}_{Br}$: X = Br, and $\mathbf{1}_{OTf}$: X= OTf) and unactivated alkynes that afford dibenzoborepins with a 7-membered ring (Fig. 1a).[13] The dibenzoborepins can be transformed into the corresponding phenanthrene derivatives by oxidative deborylation/C–C coupling.[14] When cyclooctyne, which is an activated alkyne due to a ring strain, is used in the reaction with $\mathbf{1}_{Cl}$, a multiple insertion reaction of cyclooctyne into one of the B–C bond of $\mathbf{1}_{Cl}$ occurs. For example, the reaction of $\mathbf{1}_{Cl}$ with two equivalents of cyclooctyne gives 9-membered-ring compound $\mathbf{2}_{Cl}$ quantitatively (Fig. 1a).[8] When one additional equivalent of cyclooctyne is reacted with $\mathbf{2}_{Cl}$, another insertion reaction takes place to form an 11-membered-ring intermediate, which undergoes skeletal rearrangement to give bicyclic compound $\mathbf{3}_{Cl}$ with a bridging B–Cl moiety (Fig. 1a).[8] We revealed that this rearrangement reaction is triggered by intramolecular borane-olefin proximity interactions that operate in the 11-membered-ring intermediate. Theoretical calculations suggested that strong borane-olefin proximity interactions are also present in $\mathbf{3}_{Cl}$.[8]

We were interested in the molecular structure and reactivity when the proximity interactions between the boron and olefin moieties in $\mathbf{3}_{Cl}$ are further enhanced and investigated a Cl^- abstraction reaction to generate the corresponding boron cation. Thus, $\mathbf{3}_{Cl}$ was reacted with a mesitylene complex of triethylsilylium salt $[Et_3Si(mesitylene)]^+$ $[(C_6F_5)_4B]^-$ (ESI†),[15] which is useful for the synthesis of two-coordinate borinium ion (R_2B^+) from haloborane R_2BX (X = F, Cl).[11,16] ^{1}H NMR spectral measurements of an equimolar mixture of $\mathbf{3}_{Cl}$ and $[Et_3Si(mesitylene)]^+[(C_6F_5)_4B]^-$ in deuterated ODCB (ODCB-d_4) at 25 °C showed the complete consumption of $\mathbf{3}_{Cl}$ within 5 min, and instead, the formation of a new product (Fig. 2b–d), along with chlorotriethylsilane (Fig. S1, ESI†). The generation of chlorotriethylsilane indicates that a chloride abstraction from $\mathbf{3}_{Cl}$ successfully occurred to form a cationic boron species. However, the ^{11}B NMR signal of the reaction mixture (δ = –43.5 ppm) was observed at a significantly upfield-shifted region, compared to that of $\mathbf{3}_{Cl}$ (δ = 24 ppm), as well as those reported for two-to-four-coordinate boron cations.[9,11,16] Fortunately, we could obtain high-quality single crystals of the product. Single-crystal X-ray crystallography revealed the molecular structure of the product (Fig. 3), but it was beyond our expectation. The product was a $[(C_6F_5)_4B]^-$ salt of borocenium ion $\mathbf{4}^+$ ($\mathbf{4}^+[(C_6F_5)_4B]^-$, Fig. 2a), in which a fully-substituted cyclopentadienyl (Cp) group and a fluorenyl group, which are connected to each other by a hexamethylene tether, are bonded to the cationic boron center (Figs. 1b and 3). No bond alternation is present in the Cp ring (C–C bond lengths: 1.428–1.435 Å), and the five B^+–C(Cp) bond lengths (1.764–1.796 Å) are comparable to each other. Therefore, the Cp group coordinates to the cationic boron center in a η^5 fashion,[17] which is consistent with the largely shielded ^{11}B nucleus of $\mathbf{4}^+[(C_6F_5)_4B]^-$ observed in NMR spectroscopy. The molecular structure of $\mathbf{4}^+$ is reminiscent of *ansa*-metallocene derivatives.[18] Due to this bonding feature, together with the steric protection around the cationic boron center, $\mathbf{4}^+[(C_6F_5)_4B]^-$ exhibits unusually high chemical stability to allow isolation (isolated yield of $\mathbf{4}^+[(C_6F_5)_4B]^-$: 61%, ESI†) using silica gel column chromatography under ambient conditions.

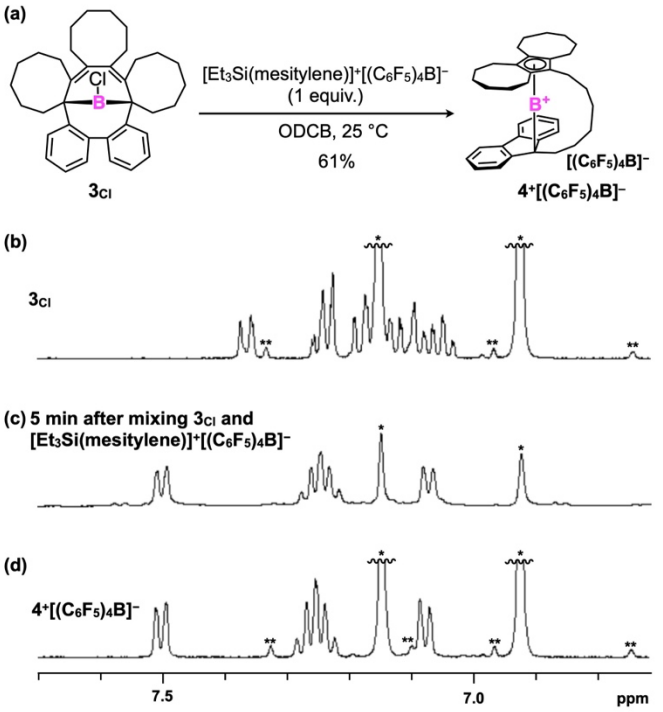

Fig. 2. (a) Intramolecular skeletal rearrangement of $\mathbf{3}_{Cl}$ into borocenium ion salt $\mathbf{4}^+[(C_6F_5)_4B]^-$ caused upon reaction with an equimolar amount of $[Et_3Si(mesitylene)]^+[(C_6F_5)_4B]^-$. ^{1}H NMR spectra (aromatic region, 400 MHz, 25 °C) in ODCB-d_4 of (b) $\mathbf{3}_{Cl}$, (c) a reaction mixture measured during the reaction of $\mathbf{3}_{Cl}$ and $[Et_3Si(mesitylene)]^+[(C_6F_5)_4B]^-$ (1 equiv.) after 5 min, and (d) $\mathbf{4}^+[(C_6F_5)_4B]^-$. Peaks denoted with asterisk (*) arise from the residual non-deuterated solvent, and those with double asterisk (**) correspond to the side bands of the solvent peaks.

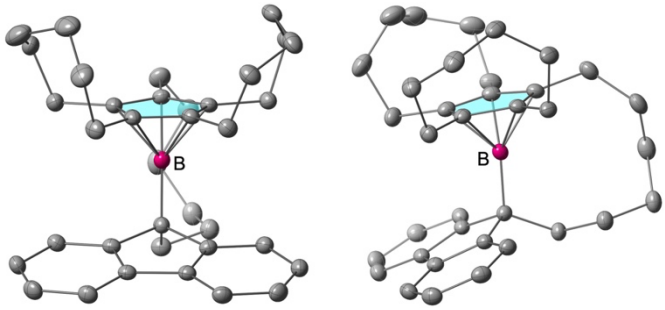

Fig. 3. X-ray crystal structure (left; top view and right; side view) of the cationic moiety of $\mathbf{4}^+[(C_6F_5)_4B]^-$ with the atomic displacement parameters set at 50% probability. Color code: boron = pink, carbon = gray. For clarity, hydrogen atoms are omitted, and the Cp ring is depicted in light blue.

The Cp ring of $\mathbf{4}^+$ has two fused 8-membered rings, which should be derived from two of the three 8-membered rings of $\mathbf{3}_{Cl}$. The remaining 8-membered ring of $\mathbf{3}_{Cl}$ most likely undergoes ring opening in the rearrangement reaction to give one of the carbon atoms (C1 atom) of the Cp ring, the bridging carbon (C8) atom of the fluorenyl group and the hexamethylene tether (Fig. 1b, carbon atoms with a red filled circle). To gain insight into the mechanism for the formation of $\mathbf{4}^+$, which is intuitively difficult

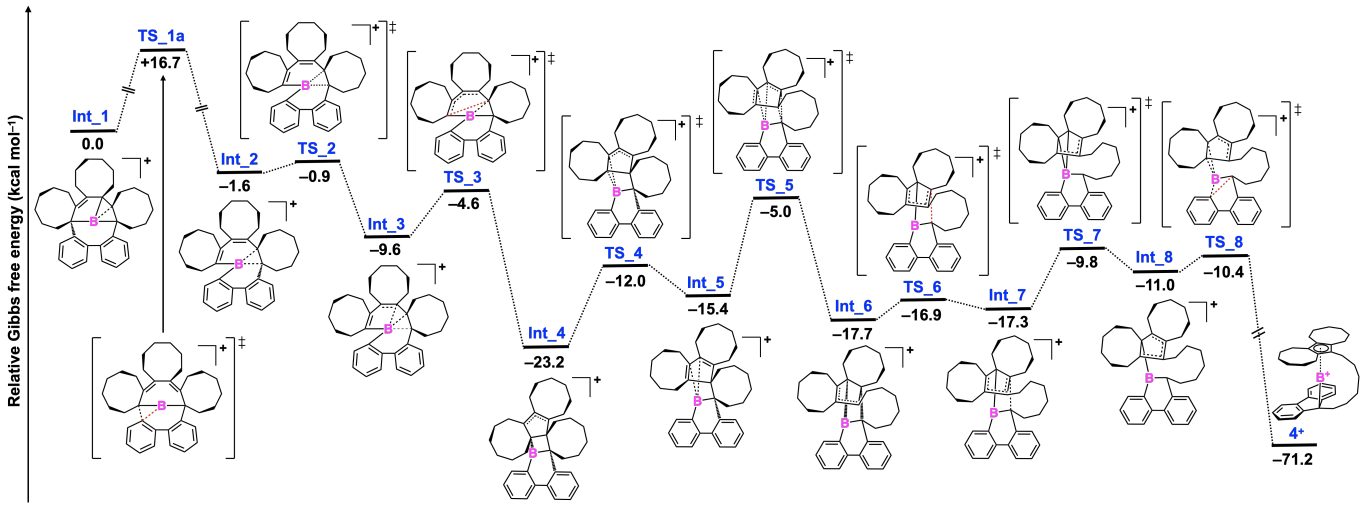

Fig. 4. Energy diagram of the most favorable pathway for the intramolecular skeletal rearrangement of a boron cation **Int_1** into borocenium ion **4**⁺ [ωB97X-D/Def2-SVPP_scrf=(smd,solvent=*o*-dichlorobenzene) level]. The energy values (in kcal mol⁻¹) relative to that of **Int_1** are shown. An unfavorable pathway obtained by the same calculation level is also shown in Fig. S2 (see also the "Computational details" section, ESI†).

to understand, we performed theoretical calculations using the global reaction route mapping (GRRM) program (ESI†).[19]

Figure 4 shows the energetically most favorable pathway for the formation of **4**⁺ from **Int_1** generated by the Cl^- abstraction reaction of $\mathbf{3_{Cl}}$. A thorough conformational search (ESI†) showed the optimized geometry of **Int_1** in which the cationic boron center strongly interacts with one of the olefin moieties in the 10-membered ring (B–C_{olefin} distances: 1.658 and 1.807 Å). **Int_2** is formed by the insertion of the boron center into a C–C_{Ar} bond through transition state **TS_1a**, where the B–C_{olefin} distances become longer (2.839 and 2.925 Å), and the boron center is arranged in proximity (1.693 Å) to an aromatic carbon atom (red broken line). **Int_2** exergonically transforms into **Int_4** while changing the interacting sites between the boron center and carbon atoms. At **TS_3** that leads to **Int_4**, a C–C bond formation (red broken line) with a distance of 2.122 Å takes place, resulting in a BC_3 4-membered ring fused with a 5-membered ring. Subsequent rearrangement from **Int_4** to **Int_6** through **TS_4**, **Int_5** and **TS_6** involves a change in the fused position of the BC_3 and 5-membered rings. Moreover, in the transformation from **Int_5** to **Int 6**, one of the 8-membered rings undergoes ring opening to form a tether moiety. Then, **Int_6** transforms into **Int_7** through a cleavage of the C–C bond (2.981 Å) at the fused position (red broken line in **TS_6**). The change in the coordination mode of the boron atom and five-membered ring from η^1 to η^5 results in the formation of **4**⁺ as the final product. Importantly, the transformation from **Int_1** to **4**⁺ is highly exergonic (–71.2 kcal mol⁻¹) and proceeds with reasonable activation barriers (the largest activation barrier: +18.2 kcal mol⁻¹ from **Int_4** to **TS_5**).

Compound **4**⁺$[(C_6F_5)_4B]^-$ is chemically very stable and remains intact even after 24 h in the presence of an excess amount of water (10 equiv.) in THF at 25 °C. However, **4**⁺$[(C_6F_5)B]^-$ readily reacted with $LiAlH_4$ (1 equiv.) in THF at 25 °C to afford neutral borane **5** with a borabicyclo[2,1,1]-hex-2-ene structure (Fig. 5), produced through the addition of H^- to the C1 carbon of **4**⁺. X-ray analysis of a single crystal of **5** grown from a hexane solution (Fig. 6a) showed that the boron and olefinic carbon atoms are arranged in proximity (B–C_{olefin} distances: 1.808 and 1.813 Å). The borane moiety is largely pyramidalized (the sum of bond angles = 311.91 °), and the boron atom is directed toward the olefinic bond. These structural features are consistent with the ^{11}B NMR observation of **5** in $CDCl_3$ at 25 °C, where the boron signal appears a substantially upfield region (–23.5 ppm).[6] While **5** is stable at room temperature in solution, it undergoes a skeletal rearrangement upon heating at 80 °C in benzene, giving rise to **6** (Fig. 5). This compound possesses a complex 3D structure in which the polycyclic borane moiety is spiro-fused with a fluorenyl group (Fig. 6b). The transformation from **5** to **6** is interesting in that it proceeds through C–B bond formations at several sp^3-carbon atoms including the C4 position in the tether moiety of **5** (Fig. 5). Here, an intramolecular dehydrogenative C–B bond formation[20] is unlikely, given that the molecular formula ($C_{36}H_{45}B$) is unchanged between **5** and **6**.

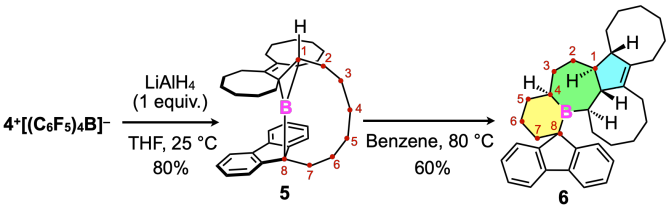

Fig. 5. Chemical transformation of **4**⁺$[(C_6F_5)B]^-$ into polycyclic boranes **5** and **6**.

In summary, we have demonstrated that a boron-containing annulenic molecule ($\mathbf{3_{Cl}}$), upon chloride abstraction to generate a cationic boron moiety, undergoes a skeletal rearrangement to form a borocenium cation (**4**⁺). Based on theoretical calculations, the boron center causes multiple C–C and C–B bonds cleavage/formation in such a way that the cationic boron center can acquire sufficient electronic stabilization. We also showed that the obtained borocenium ion (**4**⁺), upon addition

of H^- to form a neutral borane (**5**), transforms into polycyclic borane (**6**) with a complex polycyclic skeleton. Although complete understanding of the reaction mechanism is difficult at present, the selective formation from **5** to **6** implies the possibility of developing a new methodology to construct complex polycyclic aliphatic hydrocarbons by incorporating boron functionalities at an appropriate position in annulenic molecules.

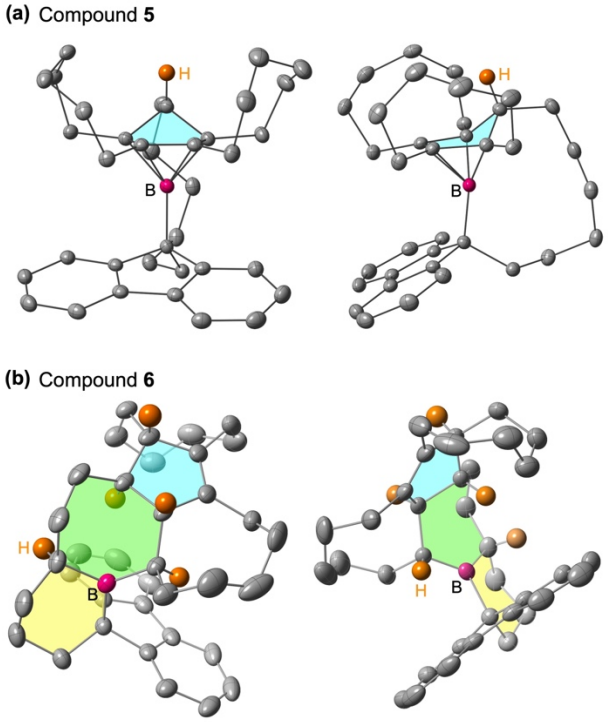

Fig. 6. X-ray crystal structures (left; top view and right; side view) of (a) **5** and (b) **6** with the atomic displacement parameters set at 50% probability. For **5**, a H atom at the C1 atom (Fig. 5) and the 5-membered ring are depicted in orange and light blue, respectively. For **6**, H atoms at the stereogenic centers are depicted in orange. The 5-, 7- and 6-membered rings at the polycyclic borane moiety are depicted in light blue, green, and yellow, respectively. Color code: boron = pink, carbon = gray.

This work was supported by a Grant-in-Aid for Transformative Research Areas (A) “Condensed Conjugation” (JSPS KAKENHI Grant Numbers JP20H05869 for Y.S. and JP20H05868 for T.F.) from MEXT, JSPS KAKENHI (JP23H01945 for Y.S.), JST ERATO (JPMJER1903 for S.M.) and the Research Program of ”Five-star Alliance” in ”NJRC Mater. & Dev.”. Y.M. is grateful to the support from a Grant-in-Aid for JSPS Fellows (JP22KJ1340).

Conflicts of interest

There are no conflicts to declare.

Notes and references

1 P. R. Jones, *J. Org. Chem.*, 1972, **37**, 1886.
2 (a) J. S. J. McCahill, G. C. Welch and D. W. Stephan, *Angew. Chem. Int. Ed.*, 2007, **46**, 4968; (b) J.-B. Sortais, T. Voss, G. Kehr, R. Fröhlich and G. Erker, *Chem. Commun.* 2009, 7417; (c) T. Voss, C. Chen, G. Kehr, E. Nauha, G. Erker and D. W. Stephan, *Chem. Eur. J.*, 2010, **16**, 3005.
3 W. A. Herrebout and B. J. van der Veken, *J. Am. Chem. Soc.*, 1997, **119**, 10446.
4 X. Zhao and D. W. Stephan, *J. Am. Chem. Soc.*, 2011, **133**, 12448.
5 (a) P. J. Fagan, E. G. Burns and J. C. Calabrese, *J. Am. Chem. Soc.*, 1988, **110**, 2979; (b) C. Balzereit, H.-J. Winkler, W. Massa and A. Berndt, *Angew. Chem. Int. Ed. Engl.*, 1994, **33**, 2306; (c) F. Ge, G. Kehr, C. G. Daniliuc and G. Erker, *J. Am. Chem. Soc.*, 2014, **136**, 68; (d) X. Su, J. J. Baker anmd C. D. Martin, *Chem. Sci.*, 2020, **11**, 126.
6 R. Oshimizu, N. Ando and S. Yamaguchi, *Angew. Chem. Int. Ed.*, 2022, **61**, e202209394.
7 (a) F. Lindl, X. Guo, I. Krummenacher, F. Rauch, A. Rempel, V. Paprocki, T. Dellermann, T. E. Stennett, A. Lamprecht, T. Brückner, K. Radacki, G. Bélanger-Chabot, T. B. Marder, Z. Lin and H. Braunschweig, *Chem. Eur. J.*, 2021**, 27**, 11226; (b) J. J. Eisch, N. K. Hota and S. Kozima, *J. Am. Chem. Soc.*, 1969, **91**, 4575; (c) J. J. Eisch and J. E. Galle, *J. Am. Chem. Soc.*, 1975, **97**, 4436; (d) J. J. Eisch, J. E. Galle, B. Shafii and A. L. Rheingold, *Organometallics*, 1990, **9**, 2342.
8 Y. Murata, K. Matsunagi, J. Kashida, Y. Shoji, C. Özen, S. Maeda and T. Fukushima, *Angew. Chem. Int. Ed.*, 2021, **60**, 14630.
9 (a) P. Kölle and H. Nöth, *Chem. Rev.*, 1985, **85**, 399; (b) W. E. Piers, S. C. Bourke and K. D. Conroy, *Angew. Chem. Int. Ed.*, 2005, **44**, 5016; (c) T. S. De Vries, A. Prokofjevs, and E. Vedejs, *Chem. Rev.*, 2012, **112**, 4246; (d) X. Tan and H. Wang, *Chem. Soc. Rev.*, 2022, **51**, 2583.
10 L. Forte, M. H. Lien, A. C. Hopkinson and D. K. Bohme, *Can. J. Chem.*, 1990, **68**, 1629.
11 N. Tanaka, Y. Shoji, D. Hashizume, M. Sugimoto and T. Fukushima, *Angew. Chem. Int. Ed.*, 2017, **56**, 5312.
12 Y. Shoji, J. Kashida and T. Fukushima, *Chem. Commun.*, 2022, **58**, 4420.
13 (a) Y. Shoji, N. Tanaka, S. Muranaka, N. Shigeno, H. Sugiyama, K. Takenouchi, F. Hajjaj and T. Fukushima, *Nat. Commun.*, 2016, **7**, 12704; (b) Y. Shoji, N. Shigeno, K. Takenouchi, M. Sugimoto and T. Fukushima, *Chem. Eur. J.*, 2018, **24**, 13223.
14 (a) Y. Shimizu, Y. Shoji, D. Hashizume, Y. Nagata and T. Fukushima, *Chem. Commun.*, 2018, **54**, 12314; (b) Y. Shoji, M. Hwang, H. Sugiyama, F. Ishiwari, K. Takenouchi, R. Osuga, J. N. Kondo, S. Fujikawa and T. Fukushima, *Mater. Chem. Front.*, 2018, **2**, 807; (c) C. Özen, Y. Shoji, T. Fukushima and S. Maeda, *J. Org. Chem.*, 2019, **84**, 1941.
15 J. B. Lambert, S. Zhang, C. L. Stern and J. C. Huffman, *Science*, 1993, **260**, 1917.
16 Y. Shoji, N. Tanaka, K. Mikami, M. Uchiyama and T. Fukushima, *Nat. Chem.*, 2014, **6**, 498.
17 (a) P. Jutzi and A. Seufert, *Angew. Chem. Int. Ed Engl.*, 1977, **16**, 41; (b) P. Jutzi, B. Krato, M. Hursthouse and A. J. Howes, *Chem. Ber.*, 1987, **120**, 565; (c) C.-T. Shen, Y.-H. Liu, S.-M. Peng and C.-W. Chiu, *Angew. Chem. Int. Ed.*, 2013, **52**, 13293; (d) Y.-F. Lin, C.-T. Shen, Y.-T. Hsiao, Y.-H. Liu, S.-M. Peng and C.-W. Chiu, *Organometallics*, 2016, **35**, 1464; (e) H.-C. Tseng, C.-T. Shen, K. Matsumoto, D.-N. Shih, Y.-H. Liu, S.-M. Peng, S. Yamaguchi, Y.-F. Lin and C.-W. Chiu, *Organometallics*, 2019, **38**, 4516.
18 E. Kirillov and J.-F. Carpentier, *Chem. Rec.*, 2021, **21**, 357.
19 (a) S. Maeda, K. Ohno and K. Morokuma, *Phys. Chem. Chem. Phys.* 2013, **15**, 3683; (b) S. Maeda, Y. Harabuchi, M. Takagi, T. Taketsugu and K. Morokuma, *Chem. Rec.*, 2016, **16**, 2232; (c) S. Maeda, Y. Harabuchi, M. Takagi, K. Saita, K. Suzuki, T. Ichino, Y. Sumiya, K. Sugiyama and Y. Ono, *J. Comput. Chem.* 2018, **39**, 233; (d) Y. Harabuchi, S. Maeda, *WIREs Comput Mol Sci.*, 2021,**11**, e1538.
20 H. Laaziri, L. O. Bromm, F. Lhermitte, R. M. Gschwind and P. Knochel, *J. Am. Chem.* Soc., 1999, **121**, 6940.